4-1999

Structural and Kinetic Studies of a Cisplatin-modified DNA Icosamer Binding to HMG1 Domain B*

Elizabeth R. Jamieson
Massachusetts Institute of Technology, ejamieso@smith.edu

Matthew P. Jacobson
Massachusetts Institute of Technology

Carmen M. Barnes
Massachusetts Institute of Technology

Christine S. Chow
Massachusetts Institute of Technology

Stephen J. Lippard
Massachusetts Institute of Technology

THE JOURNAL OF BIOLOGICAL CHEMISTRY
Vol. 274, No. 18, Issue of April 30, pp. 12346–12354, 1999

Printed in U.S.A.

Structural and Kinetic Studies of a Cisplatin-modified DNA Icosamer Binding to HMG1 Domain B*

(Received for publication, October 23, 1998, and in revised form, January 25, 1999)

Elizabeth R. Jamieson‡, Matthew P. Jacobson‡, Carmen M. Barnes, Christine S. Chow, and Stephen J. Lippard§

From the Department of Chemistry, Massachusetts Institute of Technology, Cambridge, Massachusetts 02139

The high mobility group (HMG) domain is a DNA-binding motif found in the non-histone chromosomal proteins, HMG1 and HMG2, and some transcription factors. Experimental evidence has demonstrated that HMG-domain proteins can play a role in sensitizing cells to the anticancer drug cisplatin. Fluorescence resonance energy transfer (FRET) experiments were performed in the present study to investigate structural changes that accompany complex formation between the HMG domain B of HMG1 and a cisplatin-modified, 20-base pair double-stranded DNA probe containing fluorescein and rhodamine tethered at its two ends. The binding affinity of HMG1 domain B for the cisplatin-modified DNA probe was investigated in fluorescence titration experiments, and a value of 60 ± 30 nM was determined for the dissociation constant. Single photon counting methods were employed to measure the fluorescence lifetime of the fluorescein donor in the presence and absence of HMG1 domain B. These FRET experiments revealed a distance change that was used to estimate a bend angle of 80–95° for the cisplatin-modified DNA upon protein binding. Stopped-flow fluorescence spectroscopic experiments afforded kinetic parameters for HMG1 domain B binding to the cisplatin-modified DNA probe, with k_{on} = 1.1 ± 0.1 × 10^9 M^{-1} s^{-1} and k_{off} = 30 ± 4 s^{-1}.

The long term survival for testicular cancer patients treated with *cis*-diamminedichloroplatinum(II) (cisplatin),[1] exceeds 90% (1). If the detailed mechanism of action of this anticancer drug could be determined, analogs might be designed to broaden its organotropic profile. It is generally accepted that the biological target of cisplatin is DNA, the major adducts formed being 1,2-intrastrand d(GpG) and d(ApG) cross-links involving platinum binding to the N-7 atoms of the purine bases (2). Formation of these adducts unwinds the DNA and bends it toward the major groove (3–7), blocking transcription and replication. The ability to distort DNA structure cannot fully explain the anticancer activity because the geometric isomer of cisplatin, *trans*-diamminedichloroplatinum(II), which also forms DNA adducts that modify the structure and block transcription and replication, is clinically ineffective. Efforts have therefore focused on identifying other cellular constituents that might interact specifically with cisplatin-DNA adducts to effect the antineoplastic response.

By screening human and yeast cDNA expression libraries, genes were discovered for proteins that bind specifically to cisplatin-modified DNA (8, 9). These proteins, human structure-specific recognition protein (hSSRP1) and intrastrand cross-link recognition protein (Ixr), both contain 80-amino acid peptides homologous to the DNA-binding domains of the chromosomal protein HMG1. HMG1 is the prototypical member of a family of proteins that contain such DNA-binding motifs. Most HMG-domain proteins bind specifically to the major cisplatin-DNA adducts, increasing the bend angle by up to 60°, as determined through gel mobility shift assays (10–13). HMG domain proteins shield cisplatin-DNA adducts from excision repair both in yeast cells and in human cell extracts, suggesting that they may play a role in the mechanism of action of cisplatin (11, 14, 15). SSRP1 has recently been associated with a factor involved in transcription elongation,[2] offering further clues for how these proteins might be involved in the antitumor activity.

In the present work, fluorescence resonance energy transfer (FRET) was developed as a probe for the further characterization of HMG-domain protein binding to cisplatin-modified DNA. This technique is based on the coupling of transition dipoles between two fluorescent dyes, a donor and an acceptor, attached to a macromolecule. The efficiency of the energy transfer between donor and acceptor depends on the distance between them (16). As the distance decreases, the efficiency of the energy transfer should increase. The FRET technique responds to small changes in distance in the range of 10–75 Å (16) and can reveal increased bending caused by an HMG-domain protein binding to cisplatin-modified DNA. In addition, FRET has the potential to facilitate kinetic studies of the interaction.

FRET has been used extensively to examine different types of nucleic acid structures (17–23). It has also been applied to study the structure of protein-DNA complexes (24–27). Recently, FRET techniques were used to investigate bending within a 30-bp oligonucleotide that accompanies the binding of the HMG-domain protein *Chironomus* HMG1 (26). The FRET distance measurements determined for the *Chironomus* HMG1-DNA complex enabled a bend angle of 150° to be estimated for the DNA in that complex. Experiments undertaken here similarly examine the bend angle induced when an HMG domain protein binds to cisplatin-modified DNA. A 20-bp oli-

* This work was supported in part by Grant CA34992 (to S. J. L.) from NCI, National Institutes of Health. The costs of publication of this article were defrayed in part by the payment of page charges. This article must therefore be hereby marked "*advertisement*" in accordance with 18 U.S.C. Section 1734 solely to indicate this fact.

‡ Recipient of a Department of Defense National Science and Engineering graduate fellowship.

§ To whom correspondence should be addressed: Dept. of Chemistry, Massachusetts Institute of Technology, 77 Massachusetts Ave., Cambridge, MA 02139.

[1] The abbreviations used are: cisplatin, *cis*-diamminedichloroplatinum(II); HMG, high mobility group; bp, base pair(s); FRET, fluorescence resonance energy transfer; Nd:YAG, neodymium:yttrium-aluminum-garnet; MCP-PMT, microchannel plate photomultiplier tube; HPLC, high performance liquid chromatography; W, watt(s).

[2] G. Orphanides, W.-H. Wu, W. S. Lane, M. Hampsey, and D. Reinberg, personal communication.

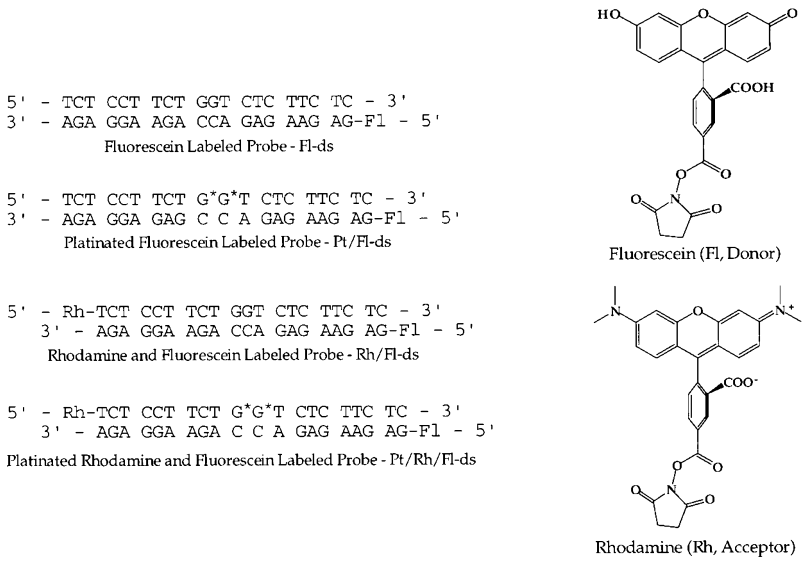

FIG. 1. **Description of the oligonucleotides used in FRET studies.** *Fl* is fluorescein, and *Rh* is rhodamine. The structures of the succinimidyl ester forms of the dyes used to label the oligonucleotides are depicted. *Fl-ds* is the fluorescein-labeled probe. *Pt/Fl-ds* is the platinated fluorescein-labeled probe. *Rh/Fl-ds* is the rhodamine- and fluorescein-labeled probe. *Pt/Rh/Fl-ds* is the platinated rhodamine- and fluorescein-labeled probe. The 1,2-intrastrand d(GpG) cisplatin adduct is denoted by *asterisks*.

gonucleotide probe modified with fluorescein as the donor and rhodamine as the acceptor was synthesized having a single cisplatin cross-link. Studies of the binding of HMG1 domain B to this FRET probe revealed the increased bending that accompanied protein-DNA complex formation, demonstrating the viability of this approach.

In addition to examining the structural change that accompanies HMG1 domain B binding, FRET was employed to monitor the kinetics of the interaction by using stopped-flow techniques. Stopped-flow fluorescence spectroscopic experiments have afforded information about the rates of binding for several other protein-DNA complexes (25, 28–31). In these studies, changes in either the intrinsic protein fluorescence or in a DNA probe containing a fluorescent label, resulting from protein-DNA complex formation, were monitored over time. The kinetics of yeast TATA-binding protein interacting with promoter DNA were revealed by FRET (25). As in the present work, these experiments used a fluorescein- and rhodamine-labeled DNA probe to follow protein-DNA complex formation. Here we provide the first quantitative information about the rates at which an HMG-domain protein binds to and dissociates from cisplatin-modified DNA.

EXPERIMENTAL PROCEDURES

Materials and Methods—Distilled, deionized water from a Milli-Q system (Millipore) was used to prepare aqueous solutions. Atomic absorption spectrometry was performed on a Varian AA1475 instrument with a GTA95 graphite furnace. High performance liquid chromatography (HPLC) was carried out by using a Waters 600E system controller equipped with either a Waters 484 or 486 detector.

Expression and Purification of Recombinant Rat HMG1 Domain B—This protein was obtained as described (13) with the following modifications. *Escherichia coli* cells were grown in LB media and lysed by sonication. After passing through the S-Sepharose column, the protein was purified by using an FPLC Superdex 75 size exclusion column (Amersham Pharmacia Biotech). The eluent for the Superdex 75 column was phosphate-buffered saline (1 mM KH_2PO_4, 10 mM Na_2HPO_4, 0.137 M NaCl, and 2.7 mM KCl, pH 7.4) with a flow rate of 0.5 ml/min.

Synthesis and Purification of Rhodamine- and Fluorescein-labeled Oligonucleotide Probes—The 20-bp oligonucleotide probes with N-TFA C6 Amino Modifier (Cruachem) attached to the 5′ end were synthesized on a Cruachem PS250 DNA synthesizer by using standard cyanoethylphosphoramidite chemistry. The crude deprotected oligonucleotides were purified by size exclusion chromatography on a G-25 Sephadex (Amersham Pharmacia Biotech) column using distilled, deionized water as the eluent. The top strand was modified with 5- and 6-carboxytetramethylrhodamine, succinimidyl ester (Molecular Probes), and the bottom strand was modified with 5- and 6-carboxyfluorescein, succinimidyl ester (Molecular Probes). The composition of the reaction mixture was 200 μM oligonucleotide, 5 mM rhodamine or fluorescein, respectively, and 0.1 M sodium carbonate buffer, pH 9.0. The reactions were stirred at room temperature for approximately 72 h. When the reactions were complete, excess unreacted dye was removed by using Centriplus 3 concentrators (Amicon) followed by dialysis (M_r cut-off 1000, Spectra/Por).

The FRET probes were purified by reverse phase HPLC on a Vydac C4 preparatory column (22 × 250 mm, 10-μm particle size) using a flow rate of 10 ml/min. Buffer A was 0.1 M NH_4OAc, and Buffer B was 0.5 M NH_4OAc in 50% CH_3CN. The gradient used was 90% Buffer A to 60% Buffer A over 30 min, followed by 60% Buffer A to 50% Buffer A over 10 min. Because the rhodamine and fluorescein dyes employed in the syntheses were a mixture of the 5- and 6-succinimidyl ester isomers, two FRET probes were observed for each synthesis in the HPLC trace. The 5-isomer was the dominant product, eluting with a greater retention time for oligonucleotides labeled with both rhodamine (~25 min) and fluorescein (~20 min), and therefore was used in the FRET experiments. Electrospray mass spectrometry was used to characterize the rhodamine-labeled top strand and fluorescein-labeled bottom strand. The molecular mass determined for the rhodamine-labeled top strand with one sodium ion was 6543.45 Da (calculated mass, 6543.03 Da), and the molecular mass determined for the fluorescein-labeled bottom strand with one sodium ion was 6819.45 Da (calculated mass, 6819.03 Da).

Reaction of Cisplatin with the Rhodamine Probe—The purified rhodamine probe was lyophilized, dissolved in distilled, deionized water, and passed through a Dowex 50 × 8–200 (Aldrich) ion exchange column to exchange the ammonium ions for sodium ions. An activated cisplatin solution was made by reaction with 1.97 mol eq of $AgNO_3$ (Aldrich) in distilled, deionized water on a shaker at room temperature overnight in the dark followed by centrifugation to remove the AgCl precipitate. The rhodamine-modified probe was platinated by addition of the activated cisplatin solution (2 eq) to a 100 μM solution of the oligonucleotide. The reaction mixture was incubated at 37 °C for ~3 h. The product was purified by HPLC, using a Dionex Nucleopac PA-100 (9 × 250 mm) preparatory column at a flow rate of 4 ml/min. It was then eluted with a gradient of 75% Buffer A (0.025 M NH_4OAc in 10% CH_3CN) to 50% Buffer A/Buffer B (0.025 M NH_4OAc, 1 M NaCl in 10% CH_3CN) over 30 min. The collected peak was dialyzed (M_r cut-off 1000, Spectra/Por) against distilled, deionized water for 48 h. Platinum atomic absorption spectroscopy revealed there to be one platinum atom per oligonucleotide strand.

Synthesis and Purification of Unlabeled Oligonucleotide Probes—A portion of the 20-bp top strand with the C6 amino modifier described above was purified by HPLC on a Dionex Nucleopac PA-100 (9 × 250 mm) preparatory column. The flow rate was 4 ml/min, and the gradient and buffers were as described above for the rhodamine probe. The collected peak was dialyzed as above. This top strand was used to make the unplatinated, fluorescein-labeled control duplex probe (Fl-ds). The unlabeled cisplatin-modified top strand was made as described previously (32) and used to make the platinated, fluorescein-labeled control duplex probe (Pt/Fl-ds).

Purification of the Fluorescent Duplex Probes—Fig. 1 shows a schematic drawing of the four different oligonucleotide duplex probes and their abbreviations. The fluorescein-labeled bottom strand was combined with unlabeled top strand, with unlabeled, cisplatin-modified top strand, with rhodamine-labeled top strand, or rhodamine-labeled, cisplatin-modified top strand to make the four different FRET probes. Equimolar amounts of the top and bottom strands were combined in a solution containing 10 mM Tris, pH 7.0, 50 mM NaCl, and 10 mM $MgCl_2$. The solution was heated to 90 °C and slowly cooled to 4 °C over several hours. The duplex DNA was purified by ion exchange HPLC to remove excess single-stranded material. A Dionex Nucleopac PA-100 (9 × 250 mm) preparatory column was used at a flow rate of 4 ml/min and a gradient of 70% Buffer A to 45% Buffer A over 30 min, followed by 45% Buffer A to 0% Buffer A over the next 10 min. Under these conditions, the duplexes eluted at ~35 min. The collected samples were dialyzed against distilled, deionized water for 48 h as above, and the resulting solutions were lyophilized to dryness. The duplex samples were redissolved in 10 mM Tris, pH 7.0, 50 mM NaCl, and 10 mM $MgCl_2$. The solutions were heated to 90 °C and slowly cooled to 4 °C over several hours. A Dionex Nucleopac PA-100 (4 × 250 mm) column was used to check the purity of the final duplex materials by analytical ion exchange HPLC.

Fluorescence Titration Experiments with HMG1 Domain B—These experiments were performed with a Hitachi F-3010 spectrofluorimeter at 25 °C. Emission spectra were recorded of both the unmodified and cisplatin-modified duplex probes labeled with both fluorescein and rhodamine in 10 mM HEPES, pH 7.0, and 200 mM NaCl solution in the presence of increasing concentrations of HMG1 domain B. The excitation wavelengths used were 480 and 550 nm, and fluorescence emission spectra were observed at 490–610 and 560–610 nm, respectively. Emission spectra obtained from exciting at 550 nm (rhodamine fluorescence only) were used to correct the data for dilution and photobleaching effects. The corrected emission spectral data at 520 nm were used to determine the dissociation constant, K_d.

K_d values were determined by plotting the change in fluorescence intensity at 520 nm, ΔF, against the total protein concentration, $[P_t]$. The data were fit to the expression described in Equation 1, where $[D_t]$ is the total oligonucleotide concentration and c is a constant that relates fluorescence intensity (I) to concentration. The average value of c was determined to be $1.8 \pm 0.5 \times 10^{-9}$ M I^{-1}. This equation is derived directly from the equilibrium mass action expression with no assumptions. The value of $[D_t]$ was set to be the concentration of DNA used in each titration experiment.

$$\Delta F = \frac{(K_d + [P_t] + [D_t]) - \sqrt{(K_d + [P_t] + [D_t])^2 - 4[D_t][P_t]}}{2c} \quad \text{(Eq. 1)}$$

Fluorescence Lifetime FRET Experiments—Time-correlated, single photon counting methods were employed to determine the fluorescence lifetime of the fluorescein in the oligonucleotide duplex probes. Light excitation was accomplished with a synchronously pumped, mode-locked, cavity-dumped picosecond dye laser system. The PUMP laser was a mode-locked Coherent Antares 76-s Nd:YAG (neodymium:yttrium-aluminum-garnet) system, which produced 22 W of 1.06-μm radiation in approximately 80-ps pulses at a repetition rate of 76.0 MHz. External frequency doubling and tripling units (CSK Optronics) were utilized to generate 1.6 W of 355-nm light, which pumped the laser dye coumarin 2 in the home-built system consisting of an extended-cavity Coherent 590 dye laser equipped with a Coherent 7220 cavity dumper. Approximately 15 mW of 450 nm light was generated at a repetition rate of 7.6 MHz, with pulse width of ~5 ps.

The sample was contained in a 1-ml fluorescence cuvette (10 × 10 mm), surrounded by an ice bath to ensure constant temperature, and irradiated within a light-tight box. The fluorescence was detected at right angles to the laser beam; no collection optics were employed, but the size of the active area on the microchannel plate photomultiplier tube (MCP-PMT; 2.0 inches in diameter) and its proximity to the sample (6 inches) ensured nearly *f*/3 collection efficiency. A combination of colored glass filters (Schott) was employed to act as a notch filter and block from the detector both scattered laser light and emission from the rhodamine on the fluorescent duplexes. This filter combination passed only a narrow band of wavelengths around 500 nm (30 nm, full width at half-maximum).

Fluorescence was detected with a two-stage MCP-PMT (Hamamatsu R1564u) having a rise time of 70 ps. The MCP-PMT output was directed through two gain 10, 2.0-GHz preamplifiers (Sonoma Instrument) and then into a constant fraction discriminator (Tennelec TC454). To take advantage of the high repetition rate of the laser, the time-to-amplitude converter (Canberra 2145) was utilized in "reverse" mode, such that pulses from the MCP-PMT provided the "start" pulse, and a time-delayed photodiode (Antel Optronics, ARX-SP, 210-ps rise time) pulse provided the "stop" pulse. The ratio of the photon detection rate to the laser repetition rate was at all times less than 1%, and usually below 0.001. The output of the time-to-amplitude converter was temporarily stored in a multichannel analyzer (Nucleus, Inc., Oak Ridge, TN) and processed on a personal computer. Typical signal integration time was 5 min for one decay measurement.

The fluorescence lifetime of the fluorescein dye was measured for 16 different samples by using the apparatus described above. The concentration of all DNA probes was 40 nM duplex in 10 mM HEPES, pH 7.0, and 200 mM NaCl. HMG1 domain B protein was added to the duplex DNA solutions, and fluorescence lifetime data were taken at 0, 1, 10, and 20 eq of added protein.

Fluorescence Lifetime Data Analysis—The fluorescein lifetime data were analyzed by using standard least-squares methods. The decays were assumed to conform to Equation 2 (33), in which $D(t)$ is the "true" decay function, $R(t)$ is the instrument response function, determined experimentally to have a full width at half-maximum of 270 ps by scattering ps laser pulses at the MCP-PMT, and C and t_o are constants.

$$I(t) = R(t + t_o) \otimes D(t) + CR(t + t_o) \quad \text{(Eq. 2)}$$

The $CR(t + t_o)$ term provides a correction for laser scatter, which was very difficult to eliminate completely, but always accounted for less than 1% of the detected photons. This correction assumes that the contribution of the scatter to the decay curve is identical to the instrument response function, that is, that all of the scatter arrives at the detector at $t = 0$. The constant t_o serves simply to set the zero of time. Both single and double exponential fits were performed (see below). For a single exponential fit, $A \exp^{(-t/\tau)}$, the total number of fitted parameters would be four: A, amplitude of decay; τ, lifetime; C, amplitude of scattered light; and t_o, zero time. The least-squares algorithm employed was a modified version of the Levenberg-Marquardt routine provided by Numerical Recipes (34).

The fluorescence lifetimes obtained from the fitting of the decay curves were used to calculate the FRET efficiencies and distances. The efficiency of energy transfer between donor and acceptor can be calculated by using Equation 3, where E is the efficiency of the energy transfer, τ_{DA} is the fluorescence lifetime of the donor in the presence of acceptor, and τ_D is the fluorescence lifetime of the donor in the absence of acceptor (16).

$$E = 1 - \tau_{DA}/\tau_D \quad \text{(Eq. 3)}$$

The distance between donor and acceptor, R, can be calculated from the FRET efficiency, E, according to Equation 4, where R_o is a characteristic distance related to the properties of the donor and acceptor at which 50% of the energy is transferred (16).

$$R^6 = R_o^6(1 - E)/E \quad \text{(Eq. 4)}$$

An R_o value of 45 Å determined for fluorescein and rhodamine (20) was used to calculate R.

Modeling the HMG1 Domain B Complex with Cisplatin-modified DNA—Fig. 2 displays the geometric model used to evaluate a bend angle for the HMG1 domain B complex with cisplatin-modified DNA. This model is based on one (20, 22) where the 20-bp oligonucleotide is represented as a cylinder with the donor and acceptor dyes extending from the ends. Vectors describing the positions of the dyes are determined as the cylinder bends and used to calculate the distance between the dyes. The hinge point of the bend is chosen as the midpoint of the central axis of the cylinder and is designated as the origin in (x, y, z) space.

The molecular modeling program QUANTA (Molecular Simulations, Inc.) was used to determine the initial positions of the donor and acceptor dyes. The first aspect examined in the model was the distance of the dyes relative to the center of the cylinder. Models of the two fluorescent dyes with their six-carbon linker chains were constructed and minimized by using the CHARMM routine contained in QUANTA. The measured distance from the center of the fluorophores to the end of the linker chain was ~1.45 nm for both dyes. If the radius of the DNA is assumed to be 1.0 nm, then the perpendicular distance of the dyes from the center of the cylinder will be 2.45 nm. The dyes may bend in toward or away from the center of the cylinder, as shown in Fig. 2. By keeping the 1.0-nm cylinder radius constant and allowing the 1.45-nm dye vector to bend, one can determine the components of the 1.45-nm vector that are perpendicular and parallel to the central cylinder axis.

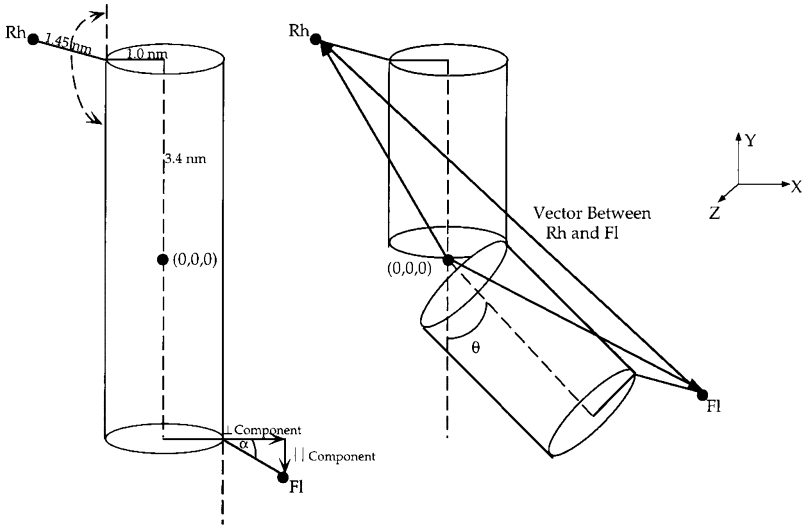

FIG. 2. **Geometric model used to calculate bend angle (θ) for fluorescence lifetime data.** The cylinder represents the 20-bp oligonucleotide. The dyes, labeled *Rh* and *Fl* for rhodamine and fluorescein, respectively, are allowed to bend toward and away from the normal to the cylinder axis at some angle, α. The model requires the determination of both the parallel ($\|$) and perpendicular ($\perp$) components of the dye vectors. The definition of the (x, y, z) axes used in the model is shown here.

The second crucial aspect of this model is the position of the fluorescent dyes relative to the bend in the DNA. In order to determine these positions, a B-form DNA model of the 20-bp oligonucleotide was constructed in QUANTA with a rhodamine dye docked onto the 5′ end of the top strand and a fluorescein dye docked onto the 5′ end of the bottom strand. A cisplatin fragment analog, *cis*-{Pt(NH_3)-($NH_2(CH_2)_nCH_3$)}$^{2+}$, was docked to the N-7 positions of the guanines in the top strand to mark the location of the 1,2-intrastrand d(GpG) cross-link and the corresponding DNA bend. Fig. 3 shows this model, which displays the positions of the fluorescent dyes relative to the cisplatin directed bend when projected down the helix axis. This view represents a slice of the cylinder in an (x, z) plane with the hinge point, (0, 0), lying in the center of the helix. The cisplatin adduct is defined to lie on the x axis. Measuring the angle between the vectors describing the position of the dyes and the x axis allows the components of these vectors along the x and z axes to be determined. In this case, the angle between the rhodamine vector and the x axis is 70°, and the angle between the rhodamine and fluorescein vectors is 200°. The latter value is in relatively good agreement with the value of 227° used by others (20).

In order to determine the vectors describing the positions of the dyes, both aspects of the model described above were combined. First, the perpendicular components of the 1.45-nm dye vectors were determined as they bend in toward and away from the cylinder. The magnitude of these components was used along with the angles determined in Fig. 3 to calculate the components of the dye vectors along the x and z axes. The component of the vector along the y axis is the sum of the parallel component of the 1.45-nm dye vector combined with the length of half the cylinder. In this case, since the hinge point is located in the center of the helix, its distance to the top of the cylinder is 3.4 nm (0.34 nm/bp for 10 bp). Once the vectors were determined for a series of rhodamine and fluorescein angles, the distance between the two dyes was calculated.

Only certain rhodamine and fluorescein angle pairs will yield the 6.4-nm distance (see "Results and Discussion") determined for the unplatinated, linear duplex in these FRET experiments. Pairs of fluorescein and rhodamine angles compatible with the 6.4-nm distance are revealed by the plot shown in Fig. 4. Although all of these allowed angle pairs yield a 6.4-nm distance for the unbent cylinder, some of the positions are preferred by the dyes. Fluorescence anisotropy experiments have indicated that fluorescein tends to have a low anisotropy value, indicative of high rotational freedom, whereas rhodamine tends to have a high anisotropy value, suggestive of an interaction between its dimethylamino groups and the phosphate backbone of the DNA (17, 20, 35). Thus, those allowed angle pairs where rhodamine has a negative angle and is bent toward the DNA may be preferred over those where the dye has a positive angle and is bent away from the DNA. It is important to keep in mind that these allowed angles are only average positional preferences. The dyes are assumed to rotate freely in the FRET equations used above to calculate distances. In the bend angle calculations described below, the preferred allowed angle pairs were examined together with positions that may be less favored.

The bending of the cylinders was performed in (x, y) space as depicted in Fig. 2 for the allowed rhodamine and fluorescein angle pairs calculated above. As the cylinder bends, the position of the rhodamine dye, and hence the vector which describes its position, was kept constant to simplify the model. The bottom half of the cylinder and the fluorescein dye moves in (x, y) space. By allowing the cylinder to bend only in an (x, y) plane, the position of the fluorescein dye relative to the z axis remains constant. The x and y components of the fluorescein vector change as the cylinder bends (Fig. 5). New fluorescein vectors for each bend angle were calculated from the altered x and y components. These new vectors were used with the rhodamine vector to determine the distance between the dyes. The bend angle that predicts the measured 5.5-nm distance (see below) between the dyes was thus estimated for the HMG1 domain B protein-DNA complex.

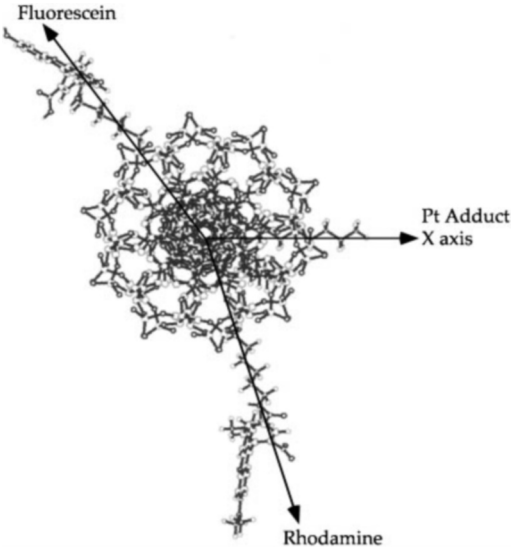

FIG. 3. **A view down the helix axis of a 20-bp B-form DNA helix.** Rhodamine is attached to the 5′-end of the top strand, and fluorescein is attached to the 5′-end of the bottom strand. A cisplatin analog is docked onto the guanines of the top strand to indicate the position of the DNA bend. The angles observed between the dyes and the x axis in this figure are used in the geometric model to help determine the vectors describing the positions of the dyes.

The above model does not take into account DNA unwinding, which might accompany platinum or protein binding. In order to do so, the initial positions of the dyes described in Fig. 3 need to be altered. The average helical twists found in the x-ray crystal structure and NMR solution structures for a 1,2-intrastrand d(GpG) cisplatin adduct were used to alter the initial positions of the dyes from Fig. 3 (6, 7, 36). The 6.6-nm distance measured for the platinated duplex without protein was used to calculate the allowed fluorophore angle positions. Those angle pairs that have the dyes separated by 6.6 nm when the DNA bends by the angles observed in the x-ray and NMR studies were used in the geometric model. With these new initial parameters, the dis-

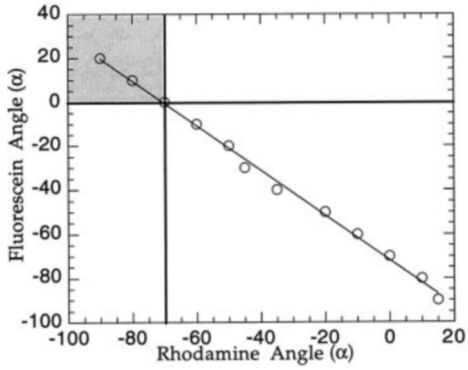

FIG. 4. **A plot of the allowed fluorescein and rhodamine angle pairs for the geometric model using the B-form DNA parameters and the 6.4-nm distance measured for the unmodified FRET probe.** There are many different allowed angle pairs. Those with rhodamine having a negative angle and fluorescein having a positive angle are preferred based on anisotropy studies and are denoted by the *shaded area*. These allowed angles are representative of those average positions in space where a 6.4-nm distance will be found.

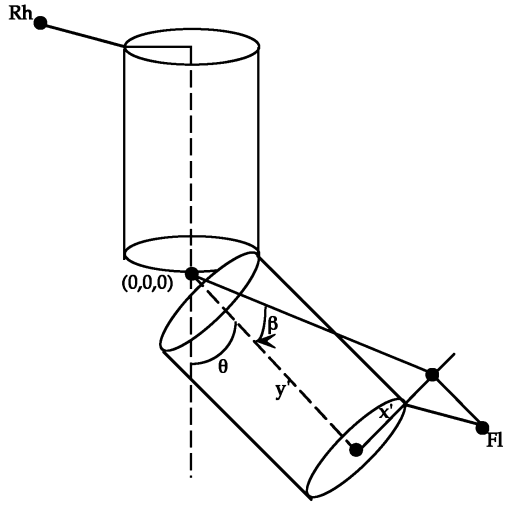

FIG. 5. **A schematic drawing of how the fluorescein dye vector is determined as the cylinder bends.** Since the cylinder bends in (x, y) space, the component of the fluorescein vector along the z axis will not change with θ. The components of the vector along the x and y axes change as follows: $(x'^2 + y'^2)\cos((90 + \beta) - \theta)$ (for x axis) and $-(x'^2 + y'^2)\sin((90 + \beta) - \theta)$ (for y axis). The angle, β, is equal to the $\tan^{-1}(x'/y')$.

tances between the dyes as the cylinder bends were calculated as described above.

Stopped-flow Kinetic Studies with HMG1 Domain B—These experiments were performed with a Hi-Tech SF-61 DX2 double mixing stopped-flow apparatus at 4 °C. HMG1 domain B was combined with 25 nM unmodified or cisplatin-modified duplex probes labeled with both fluorescein and rhodamine in 10 mM HEPES, pH 7, 200 mM NaCl. Pseudo-first order kinetic conditions were maintained by using at least a 5-fold excess of protein in all experiments. The excitation wavelength was 480 nm. A GG495 glass cut-off filter and a Wratten gel filter no. 58 (Eastman Kodak) were placed over the exit to the photomultiplier tube. This filter pair served to block rhodamine fluorescence and transmit the FRET-induced fluorescein fluorescence change.

Concentration-dependent studies were performed with the cisplatin-modified probe and HMG1 domain B to determine the rate constants for the binding and dissociation of this protein-DNA complex. In these experiments, the protein concentration was varied from 0.125 to 1 μM. Multiple shots were taken at each protein concentration. The observed rate constants for the protein concentrations were determined by fitting individual traces with the KinetAssyst software package (Hi-Tech) and averaging the results. The observed rate constant, k_{obs}, was plotted against the total protein concentration, $[P_t]$. The resulting linear plot is described by Equation 5, where k_{on} is the second-order rate constant for protein binding and k_{off} is the first-order rate constant for the dissociation of the protein-DNA complex.

$$k_{obs} = k_{on}[P_t] + k_{off} \quad \text{(Eq. 5)}$$

In these experiments, the least-squares fit of each point was weighted by the number of shots averaged to determine the k_{obs} value. The rate constants, determined in Equation 5, were used to calculate a dissociation constant, K_d, for the protein-DNA complex according to Equation 6.

$$K_d = k_{off}/k_{on} \quad \text{(Eq. 6)}$$

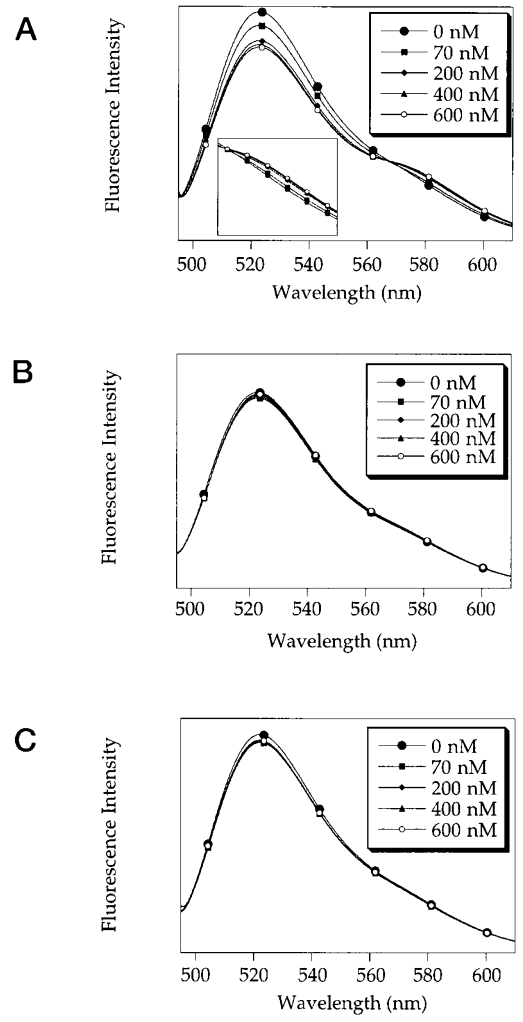

FIG. 6. **Emission spectra from fluorescence titration experiments.** *A*, Pt/Rh/Fl-ds with increasing HMG1 domain B; *B*, Rh/Fl-ds with increasing HMG1 domain B; *C*, Pt/Rh/Fl-ds titrated with distilled, deionized water. The *inset* to *A* shows an enlargement of the spectral region from 565 to 600 nm to highlight the increase in rhodamine fluorescence.

RESULTS AND DISCUSSION

Determination of K_d from Steady-state Fluorescence Titration Experiments—Fig. 6 shows emission spectra from three different fluorescence titration experiments in which the fluorescein dye was excited at 480 nm and emission spectra were recorded from 490 to 610 nm. The fluorescein emission maximum occurs at 520 nm, and the rhodamine emission maximum at 580 nm. *Panel A* of Fig. 6 presents the results of titrating Pt/Rh/Fl-ds with increasing amounts of HMG1 domain B. The *inset* enlarges the spectral region from 565 to 600 nm. *Panel B* displays the unplatinated Rh/Fl-ds sample with increasing amounts of HMG1 domain B, and *panel C* shows the platinated Pt/Rh/Fl-ds probe titrated with distilled, deionized water instead of protein. The results clearly demonstrate that significant spectral

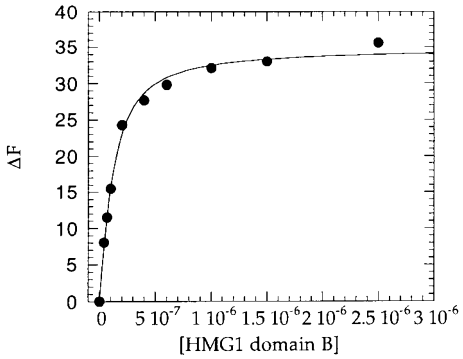

FIG. 7. **Determination of K_d from titration data.** The data shown are for a single titration experiment fit to Equation 1. Several experiments were carried out, and the results averaged to determine the final dissociation constant value.

changes occur only when the platinated probe is titrated with protein.

From the decrease in the fluorescence intensity at 520 nm for the fluorescein donor and the increase in the fluorescence emission of the rhodamine acceptor dye at 580 nm with increasing protein concentration (*inset*), it is clear that FRET occurs. We ascribe this result to protein-induced bending of the platinated DNA. The spectral observed changes were used to determine the dissociation constant of this protein-DNA complex. The change in fluorescence intensity at 520 nm (ΔF) is directly related to the concentration of the protein-DNA complex, assumed to have a 1:1 stoichiometry. Plots of ΔF *versus* $[P_t]$ (Fig. 7) were fit by least squares to Equation 1, affording an average dissociation constant of 60 ± 30 nM.

Recently, a series of cisplatin-modified 15-bp oligonucleotides were reported to have a range of dissociation constants for the HMG1 domain B complex of 50–1300 nM (37), as determined by gel mobility shift assays. The value of 60 ± 30 nM determined here falls within this range, but is ~8 times smaller than the one previously determined for the identical 20-bp oligonucleotide by gel mobility shift assay (13). This discrepancy is ascribed to differences in the experimental conditions, the present experiments being performed at a different temperature and with different buffer conditions than in the gel mobility shift assay.

Duplex End-to-end Distance from Fluorescein Fluorescence Lifetime Measurements—Fluorescence emission decay curves were obtained and the data were analyzed as described above. An example of a fitted fluorescence emission decay curve is presented in the *upper panel* of Fig. 8. The *bottom panel* of this figure depicts the weighted residuals of the fit, $(I_{obs} - I_{calc})/\sigma_i$, where σ_i is the standard deviation associated with I_{obs}, $\sigma_i = (I_{obs})^{0.5}$. Most of the weighted residuals lie within two standard deviations. The fluorescence lifetime values obtained from fitting the decay curves are presented in Table I.

The data in Table I show that, for the fluorescein-labeled (Fl-ds), platinated fluorescein-labeled (Pt/Fl-ds), and rhodamine- and fluorescein-labeled (Rh/Fl-ds) duplex oligonucleotides, the fluorescein fluorescence lifetime either remains the same or increases slightly with increasing concentrations of HMG1 domain B. The data for the platinated oligonucleotide with rhodamine and fluorescein (Pt/Rh/Fl-ds) clearly display a different trend. The lifetime of fluorescein in this probe in the absence of added protein is slightly increased from that of the Rh/Fl-ds duplex, presumably due to DNA unwinding and bending upon platination. When increasing concentrations of HMG1 domain B were added, there was a significant decrease in fluorescence lifetime of the fluorescein label. This difference in lifetimes is apparent in the decay curves plotted in Fig. 9, the log format of which emphasizes the effect. In this figure, the Pt/Fl-ds and Pt/Rh/Fl-ds probes with no protein are compared with the Pt/Rh/Fl-ds probe with 20 eq of added HMG1 domain B. The longest fluorescence lifetime is for fluorescein in the Pt/Fl-ds sample. The lifetime shortens when the acceptor dye is present, and with 20 eq of HMG1 domain B the Pt/Rh/Fl-ds probe exhibits the shortest fluorescence lifetime. The changes are consistent with FRET induced by protein binding and bending the platinated DNA.

The fluorescence lifetime values were used to calculate FRET efficiency (E) and the distance (R) between the dyes in these different samples. Table II shows the results computed by Equations 3 and 4 for the Rh/Fl-ds and Pt/Rh/Fl-ds probes. As expected from the lifetime studies, the Rh/Fl-ds samples exhibit only a small increase in FRET efficiency with increas-

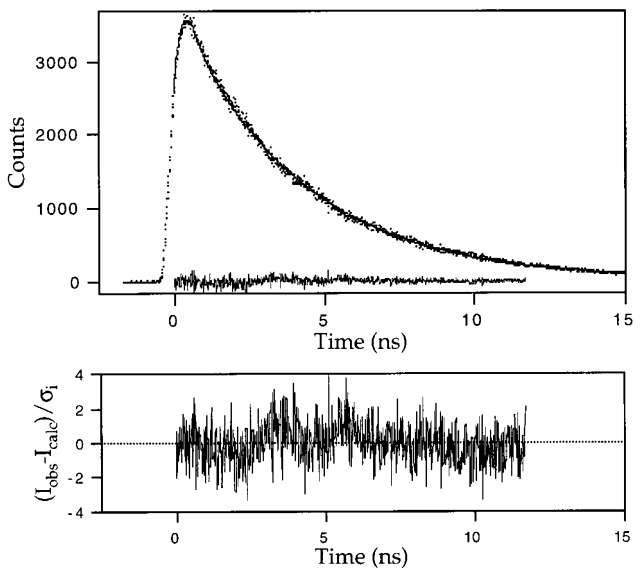

FIG. 8. **Example of a fitted fluorescence emission decay curve.** Data were fitted as described under "Experimental Procedures." The *upper panel* shows the fitted decay curve, and the *lower panel* depicts the weighted residuals of the fit.

TABLE I
Fluorescein lifetime values obtained from single exponential fits of the single photon counting data[a]

Sample[b]	Fluorescein lifetime
	ns
Fl-ds	4.03 (1)
Fl-ds + 1 eq HMGdomB	4.02 (1)
Fl-ds + 10 eq HMGdomB	4.10 (1)
Fl-ds + 20 eq HMGdomB	4.14 (1)
Pt/Fl-ds	4.03 (1)
Pt/Fl-ds + 1 eq HMGdomB	3.99 (1)
Pt/Fl-ds + 10 eq HMGdomB	4.04 (2)
Pt/Fl-ds + 20 eq HMGdomB	4.12 (1)
Rh/Fl-ds	3.59 (1)
Rh/Fl-ds + 1 eq HMGdomB	3.64 (2)
Rh/Fl-ds + 10 eq HMGdomB	3.62 (1)
Rh/Fl-ds + 20 eq HMGdomB	3.62 (1)
Pt/Rh/Fl-ds	3.65 (1)
Pt/Rh/Fl-ds + 1 eq HMGdomB	3.63 (1)
Pt/Rh/Fl-ds + 10 eq HMGdomB	3.24 (1)
Pt/Rh/Fl-ds + 20 eq HMGdomB	3.18 (1)

[a] Numbers in parentheses are standard deviations in the last significant digit. Oligonucleotide probe concentrations were 40 nM in all samples.

[b] Fl-ds is the fluorescein-only-labeled probe. Pt/Fl-ds is the platinated, fluorescein-only-labeled probe. Rh/Fl-ds is the probe labeled with both fluorescein and rhodamine. Pt/Rh/Fl-ds is the platinated probe labeled with both fluorescein and rhodamine.

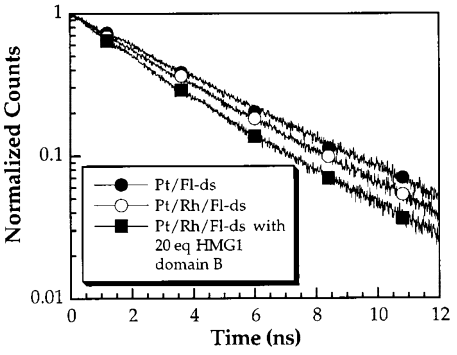

FIG. 9. **Normalized fluorescence lifetime decay curves for some selected samples.** Curves for Pt/Fl-ds, Pt/Rh/Fl-ds, and Pt/Rh/Fl-ds with 20 eq HMG1 domain B are depicted. Plots are shown in log scale for clarity.

TABLE II
FRET efficiency and distance data

Numbers in parentheses are standard deviations in the last significant digit.

Sample[a]	FRET efficiency	Distance (R)
	E	*nm*
Rh/Fl-ds	0.11 (1)	6.4 (1)
Rh/Fl-ds + 1 eq HMGdomB	0.09 (1)	6.6 (1)
Rh/Fl-ds + 10 eq HMGdomB	0.12 (1)	6.3 (1)
Rh/Fl-ds + 20 eq HMGdomB	0.12 (1)	6.3 (1)
Pt/Rh/Fl-ds	0.09 (1)	6.6 (1)
Pt/Rh/Fl-ds + 1 eq HMGdomB	0.09 (1)	6.6 (1)
Pt/Rh/Fl-ds + 10 eq HMGdomB	0.20 (2)	5.7 (1)
Pt/Rh/Fl-ds + 20 eq HMGdomB	0.23 (2)	5.5 (1)

[a] Rh/Fl-ds is the probe labeled with both fluorescein and rhodamine. Pt/Rh/Fl-ds is the platinated probe labeled with both fluorescein and rhodamine.

ing protein concentrations, corresponding to a decrease in distance of only ~0.1 nm, from 6.4 to 6.3 nm. The Pt/Rh/Fl-ds samples, however, show a dramatic increase in FRET efficiency, from 0.09 to 0.23 with increasing protein concentrations. This result reflects a change in distance between donor and acceptor of −1.1 nm, from 6.6 to 5.5 nm. The 17% decrease may be attributed to protein binding and concomitant DNA bending.

Most of the fluorescence decay curves were adequately fit to a single-exponential function. The Pt/Rh/Fl-ds samples containing excess HMG1 domain B deviated the most from single exponential behavior. Double-exponential fits were therefore investigated, the results of which are reported in Table III. The double-exponential fits at the higher concentrations of protein afford fluorescence lifetimes of approximately 5.0 and 2.4 ns. One possible explanation for this behavior is that the lifetimes reflect contributions from both bound and free DNA (26). In this interpretation, the shorter lifetime value would represent the protein bound DNA, and the ~5.0-ns lifetime, the free DNA. Using this value for the bound DNA, the FRET efficiency increases from 0.09 to ~0.4, corresponding to a distance change of 1.9 nm and indicating greater DNA bending (~90–120°). The ~5.0-ns lifetime value for the free DNA, however, is much longer than any observed for fluorescein in the single exponential fits of the data, making this explanation unsatisfactory. In addition, even in the most extreme cases, the discrepancy between the observed data and the single-exponential fits was fairly small, and the double-exponential fits improved chi-squared by at most ~40% over the single exponential fits. Therefore, in the absence of an adequate explanation for the weakly multiexponential behavior of some of the decays, we use the single-exponential decay values to calculate FRET efficiency in all cases.

TABLE III
Double exponential fits to data for Pt/Rh/Fl-ds samples with excess HMG1 domain B

Numbers in parentheses are standard deviations in the last significant digit.

Sample	Pre-exponential	Lifetime	Efficiency	Distance
		ns	*E*	*nm*
Pt/Rh/Fl-ds + 10 eq	3200 ± 500	2.4 (2)	0.41 (3)	4.8 (1)
HMGdomB	1300 ± 600	4.9 (7)		
Pt/Rh/Fl-ds + 20 eq	3700 ± 500	2.3 (2)	0.44 (4)	4.7 (1)
HMGdomB	1700 ± 600	4.6 (5)		

Modeling the Bending of the HMG1 Domain B–Cisplatin-modified DNA Complex—The distances determined from the FRET lifetime experiments were used to estimate a bend angle for the protein-DNA complex. Figs. 2–5 describe the geometric model used along with the distances determined from the single-exponential fits to compute a bend angle for the HMG1 domain B complex with cisplatin-modified DNA. In the first case examined, geometric parameters for normal B-form DNA were used along with the distance determined for the unmodified FRET probe. The bending of the cylinder, which created a 5.5-nm separation between the fluorophores, occurred in the range of 90–100°. The geometric model was then altered to examine the effects of DNA unwinding on the estimated bend angle. A smaller bend of ~70–85° obtained when the helical twist and bend angle range from the x-ray crystal structure were employed is judged to be less reliable because of duplex-duplex packing interactions in the solid state that render these values less relevant to the solution structure (6). Using the average helical twist and bend angle range determined for the NMR solution structures of duplex DNA containing a 1,2-intrastrand d(GpG) cisplatin adduct (7, 36), the 5.5-nm distance occurred when the DNA was bent by ~80–95°. The ~60–80° bend and underwinding of the platinated DNA duplex push the limits of the geometric model used to estimate a bend angle from the FRET data. In particular, when compared with models where the helical twist and bend angles from B-form DNA were used, the number of allowed fluorescein and rhodamine angles were significantly fewer. Moreover, none of the angle pairs, which yielded a 6.6-nm distance, was in the preferred position where rhodamine bends toward the DNA. Hence, it is important to examine these estimated bend angles and see how they compare with ones determined by other techniques.

The ~80–95° range estimated using helical twists and bend angles from the NMR studies of the 1,2-intrastrand d(GpG) cisplatin adduct seems reasonable, based on the results of NMR solution studies of DNA complexes with other HMG-domain proteins (38, 39). In the SRY NMR structure, the DNA is bent by ~70–80° (39), and for LEF-1, the DNA is bent by ~117° (38). The bend angle range estimated with our geometric model falls within the range determined in these NMR studies. The DNA bending caused by the formation of complexes with HMG-domain proteins has also been investigated by gel mobility shift assays (12) and x-ray crystallography.[3] The bend angle determined in gel shift studies for the HMG1 domain B complex with a cisplatin-modified DNA probe was ~65–74° (12). X-ray crystallography shows the bend angle for a cisplatin-modified DNA probe bound to HMG1 domain A to be ~61°.[3] Both of these values are smaller than what was estimated from our geometric models.

The discrepancy between the present bend angle value and that for other complexes of HMG-domain proteins with plati-

[3] U.-M. Ohndorf, M. A. Rould, Q. He, C. O. Pabo, and S. J. Lippard, personal communication.

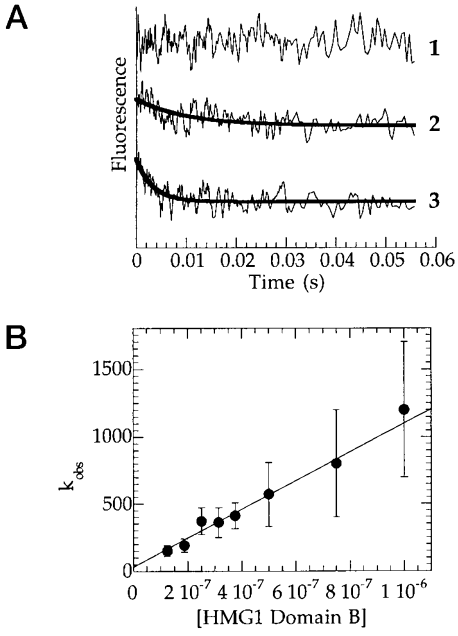

FIG. 10. **Stopped-flow kinetic experiments with HMG1 domain B.** *Panel A* displays individual shots. *Curve 1* is the unmodified duplex probe with 500 nM HMG1 domain B. *Curves 2* and *3* show the cisplatin-modified duplex probe with 188 and 375 nM HMG1 domain B, respectively. *Panel B* is a plot of the concentration dependent data fitted to Equation 6, from which were determined k_{on} and k_{off} values of $1.1 \pm 0.1 \times 10^9$ M^{-1} s^{-1} and 30 ± 4 s^{-1}, respectively.

nated DNA is ascribed in part to differences in experimental methods. For example, crystal packing forces can affect the bend angle in an x-ray crystal structure compared with the FRET studies, where the complex is free in solution. Another possible contribution to the larger bend angle, estimated here, could be the different DNA sequence employed. Recent work indicates that the sequence context surrounding the 1,2-intrastrand d(GpG) cisplatin adduct modulates the binding affinity of HMG-domain proteins (37) and may influence the ability of the DNA to bend when an HMG-domain protein binds (6, 37). In the FRET study, the platinated sequence was TG^*G^*T, whereas the sequence in the gel shift assay study was AG^*G^*C and in the x-ray study, TG^*G^*A, where G^* denotes the modified nucleotide. The presence of an additional surrounding A/T base pair may increase the bendability of the DNA used in the FRET experiment compared with the gel shift study owing to the fewer number of hydrogen bonds (37). From these considerations, we conclude that the 80–95°-bend angle range estimated from the geometric model for these FRET studies is reasonable.

Rate of HMG1 Domain B Binding to Cisplatin-modified DNA: Stopped-flow Kinetic Experiments—Stopped-flow kinetic experiments were performed with both the unmodified and cisplatin-modified DNA probes containing fluorescent labels. Fig. 10 portrays results from some of these experiments. In *panel A* are presented data from some of the individual shots. *Curve 1* shows the unmodified probe with 500 nM HMG1 domain B. No fluorescence change is observed for this sample. *Curves 2* and *3* exhibit the cisplatin-modified probe in the presence of 188 and 375 nM HMG1 domain B, respectively. Here, a decrease in the fluorescein fluorescence is observed over time that is ascribed to protein binding and concomitant bending of the DNA. Although the protein concentration is always in excess, in order to maintain pseudo-first order conditions, the two different concentrations of protein shown in *panel A* clearly demonstrate that the rate decrease depends on protein concentration.

A concentration-dependent study of the observed rate constants was carried out for the cisplatin-modified probe binding to HMG1 domain B in order to determine the rate constants for binding and the dissociation of the complex. The results from these experiments are illustrated in *panel B* of Fig. 10. A fit of the data to Equation 5 gives a second-order rate constant for binding, k_{on}, of $1.1 \pm 0.1 \times 10^9$ M^{-1} s^{-1} and a first-order rate constant for the dissociation of the protein-DNA complex, k_{off}, 30 ± 4 s^{-1} ($t_{1/2} = 0.023$ s). The dissociation constant, K_d, determined from these rate constants using Equation 6 is 27 ± 4 nM, which is in agreement with the value determined in the fluorescence titration experiments.

The results of these experiments provide the first information about the kinetics of HMG-domain proteins binding to cisplatin-modified DNA. Very little kinetic information is available for HMG-domain protein binding to DNA in general. Data that are available were obtained through competition kinetic gel shift experiments, and not by direct measurement of the binding event, as accomplished in the present FRET study (40). The kinetics of binding of an HMG-domain protein to cisplatin-modified DNA is potentially important for understanding its possible role in sensitizing cells to the drug. Recent experiments examined the interactions of RPA, a protein involved in DNA damage recognition in the nucleotide excision repair pathway, and HMG1 to cisplatin-modified DNA (41). The results of these experiments revealed that, when both proteins were present, HMG1 selectively bound the platinated DNA (41). One possible explanation for this result is that HMG1 binding to cisplatin-modified DNA occurs at a rate faster than that of RPA binding and that kinetics controls the competition (41). The k_{on} value for HMG1 determined here, which is near the diffusion limit, is consistent with such an explanation.

In conclusion, the present study illustrates the utility of the FRET technique for investigating the structure and dynamics of proteins binding to platinated DNA. The method offers the potential for measuring distances and binding rates in solution and has an advantage over x-ray crystallographic and gel mobility shift approaches, which do not permit solution studies to be carried out over a wide range of conditions, such as ionic strength or pH. FRET experiments can also be performed using low concentrations of material, an advantage over NMR spectroscopy. Finally, it is relatively easy to alter the nature of the fluorescent label and to examine FRET distance changes with different oligonucleotide sequences. By varying the length and studying a series of oligonucleotide probes, more elaborate models may be constructed to examine changes in the helical parameters of the DNA (20, 42).

Acknowledgments—Fluorescence lifetime experiments were carried out in the Harrison Spectroscopy Laboratory at the Massachusetts Institute of Technology. We thank Dr. George T. Gassner for help with the stopped-flow experiments, Dr. John S. Wishnok in the MIT Division of Toxicology mass spectrometry laboratory for electrospray mass spectrometric characterization of fluorescently labeled oligonucleotides, and Johnson Matthey for a gift of cisplatin.

REFERENCES

1. Pil, P., and Lippard, S. J. (1997) in *Encyclopedia of Cancer* (Bertino, J. R., ed) Vol. 1, pp. 392–410, Academic Press, San Diego, CA
2. Lepre, C. A., and Lippard, S. J. (1990) in *Nucleic Acids and Molecular Biology* (Eckstein, F., and Lilley, D. M. J., eds) Vol. 4, pp. 9–38, Springer-Verlag, Heidelberg
3. Bellon, S. F., and Lippard, S. J. (1990) *Biophys. Chem.* **35,** 179–188
4. Bellon, S. F., Coleman, J. H., and Lippard, S. J. (1991) *Biochemistry* **30,** 8026–8035
5. Takahara, P. M., Rosenzweig, A. C., Frederick, C. A., and Lippard, S. J. (1995) *Nature* **377,** 649–652
6. Takahara, P. M., Frederick, C. A., and Lippard, S. J. (1996) *J. Am. Chem. Soc.* **118,** 12309–12321
7. Gelasco, A., and Lippard, S. J. (1998) *Biochemistry* **37,** 9230–9239
8. Toney, J. H., Donahue, B. A., Kellett, P. J., Bruhn, S. L., Essigmann, J. M., and Lippard, S. J. (1989) *Proc. Natl. Acad. Sci. U. S. A.* **86,** 8328–8332
9. Bruhn, S. L., Pil, P. M., Essigmann, J. M., Housman, D. E., and Lippard, S. J.

(1992) *Proc. Natl. Acad. Sci. U. S. A.* **89,** 2307–2311
10. Pil, P. M., and Lippard, S. J. (1992) *Science* **256,** 234–237
11. Brown, S. J., Kellett, P. J., and Lippard, S. J. (1993) *Science* **261,** 603–605
12. Chow, C. S., Whitehead, J. P., and Lippard, S. J. (1994) *Biochemistry* **33,** 15124–15130
13. Chow, C. S., Barnes, C. M., and Lippard, S. J. (1995) *Biochemistry* **34,** 2956–2964
14. Huang, J.-C., Zamble, D. B., Reardon, J. T., Lippard, S. J., and Sancar, A. (1994) *Proc. Natl. Acad. Sci. U. S. A.* **91,** 10394–10398
15. McA'Nulty, M. M., and Lippard, S. J. (1996) *Mutat. Res.* **362,** 75–86
16. Selvin, P. R. (1995) *Methods Enzymol.* **246,** 300–334
17. Clegg, R. M., Murchie, A. I. H., Zechel, A., Carlberg, C., Diekmann, S., and Lilley, D. M. J. (1992) *Biochemistry* **31,** 4846–4856
18. Cardullo, R. A., Agrawal, S., Flores, C., Zamecnik, P. C., and Wolf, D. E. (1988) *Proc. Natl. Acad. Sci. U. S. A.* **85,** 8790–8794
19. Murchie, A. I. H., Clegg, R. M., von Kitzing, E., Duckett, D. R., Diekmann, S., and Lilley, D. M. J. (1989) *Nature* **341,** 763–766
20. Clegg, R. M., Murchie, A. I. H., Zechel, A., and Lilley, D. M. J. (1993) *Proc. Natl. Acad. Sci. U. S. A.* **90,** 2994–2998
21. Eis, P. S., and Millar, D. P. (1993) *Biochemistry* **32,** 13852–13860
22. Gohlke, C., Murchie, A. I. H., Lilley, D. M. J., and Clegg, R. M. (1994) *Proc. Natl. Acad. Sci. U. S. A.* **91,** 11660–11664
23. Mahtab, R., Rogers, J. P., Singleton, C. P., and Murphy, C. J. (1996) *J. Am. Chem. Soc.* **118,** 7028–7032
24. Heyduk, T., and Lee, J. C. (1992) *Biochemistry* **31,** 5165–5171
25. Parkhurst, K. M., Brenowitz, M., and Parkhurst, L. J. (1996) *Biochemistry* **35,** 7459–7465
26. Heyduk, E., Heyduk, T., Claus, P., and Wiśniewski, J. R. (1997) *J. Biol. Chem.* **272,** 19763–19770
27. Ozaki, H., Iwase, N., Sawai, H., Kodama, T., and Kyogoku, Y. (1997) *Biochem. Biophys. Res. Commun.* **231,** 553–556
28. Perez-Howard, G. M., Weil, P. A., and Beechem, J. M. (1995) *Biochemistry* **34,** 8005–8017
29. Jia, Y., Kumar, A., and Patel, S. S. (1996) *J. Biol. Chem.* **271,** 30451–30458
30. Sha, M., Ferré-D'Amaré, A. R., Burley, S. K., and Goss, D. J. (1995) *J. Biol. Chem.* **270,** 19325–19329
31. Urbanke, C., and Schaper, A. (1990) *Biochemistry* **29,** 1744–1749
32. Poklar, N., Pilch, D. S., Lippard, S. J., Redding, E. A., Dunham, S. U., and Breslauer, K. J. (1996) *Proc. Natl. Acad. Sci. U. S. A.* **93,** 7606–7611
33. O'Connor, D. V., and Phillips, D. (1984) *Time-correlated Single Photon Counting*, Academic Press, London
34. Press, W. H., Teukolsky, S. A., Vetterling, W. T., and Flannery, B. P. (1992) *Numerical Recipes in FORTRAN*, 2nd Ed., Cambridge University Press, Cambridge, United Kingdom
35. Tuschl, T., Gohlke, C., Jovin, T. M., Westhof, E., and Eckstein, F. (1994) *Science* **266,** 785–789
36. Yang, D., van Boom, S. S. G. E., Reedijk, J., van Boom, J. H., and Wang, A. H.-J. (1995) *Biochemistry* **34,** 12912–12920
37. Dunham, S. U., and Lippard, S. J. (1997) *Biochemistry* **36,** 11428–11436
38. Love, J. J., Li, X., Case, D. A., Giese, K., Grosschedl, R., and Wright, P. E. (1995) *Nature* **376,** 791–795
39. Werner, M. H., Huth, J. R., Gronenborn, A. M., and Clore, G. M. (1995) *Cell* **81,** 705–714
40. Giese, K., Amsterdam, A., and Grosschedl, R. (1991) *Genes Dev.* **5,** 2567–2578
41. Patrick, S. M., and Turchi, J. J. (1998) *Biochemistry* **37,** 8808–8815
42. Jares-Erijman, E. A., and Jovin, T. M. (1996) *J. Mol. Biol.* **257,** 597–617